Brief communication: Collapse of 4 Mm^3 ice from a cirque glacier in the Central Andes of Argentina

Daniel Falaschi[1,2], Andreas Kääb[3], Frank Paul[4], Takeo Tadono[5], Juan Antonio Rivera[2], Luis Lenzano[1,2]

1. Departamento de Geografía, Facultad de Filosofía y Letras, Universidad Nacional de Cuyo, Mendoza, 5500, Argentina
2. Instituto Argentino de Nivología, Glaciología y Ciencias Ambientales, Mendoza, 5500, Argentina
3. Department of Geosciences, University of Oslo, Oslo, 0371, Norway
4. Department of Geography, University of Zürich, Zürich, 8057, Switzerland
5. Earth Observation research Center, Japan Aerospace Exploration Agency, Tsukuba, 305-8505, Japan

Correspondence to: Daniel Falaschi (dfalaschi@mendoza-conicet.gov.ar)

Abstract. Among glacier instabilities, collapses of large parts of low-angle glaciers are a striking, exceptional phenomenon. So far, merely the 2002 collapse of Kolka Glacier in the Caucasus Mountains and the 2016 twin detachments of the Aru glaciers in western Tibet have been well documented. Here we report on the previously unnoticed collapse of an unnamed cirque glacier in the Central Andes of Argentina in March 2007. Although of much smaller ice volume, this 4.2 ±0.6 × 10^6 m^3 collapse in the Andes is similar to the Caucasus and Tibet ones in that the resulting ice avalanche travelled a total distance of ~2 km over a surprisingly low angle of reach (~5°).

1 Introduction

On steep glacier fronts, icefalls, and hanging glaciers (usually >30º steep), glacier instabilities in the form of ice break-offs and avalanches of varying size and magnitude are common and have been noted everywhere around the globe (Faillettaz et al., 2015). The current WGMS '*special events*' database lists in fact a total of 110 ice avalanche events worldwide (WGMS, 2017). Such gravitational ice failures can be a normal process of ablation of steep glaciers, but extraordinary events can be triggered by seismic events and changes in the ice thermal regime or in topographic or atmospheric conditions (Faillettaz et al., 2015). Typical volumes of ice avalanches from steep glaciers are in the order of up to several 10^5 m^3, with extraordinary event volumes of up to several 10^6 m^3. Yet the detachment of large portions of low-angle glaciers is a much less frequent process, and has so far only been documented in detail for the 130 × 10^6 m^3 avalanche released from the Kolka Glacier in the Russian Caucasus in 2002 (Evans et al., 2009), and the recent 68 ±2 × 10^6 m^3 and 83 ±2 × 10^6 m^3 collapses of two adjacent glaciers in the Aru range in the Tibetan Plateau (Tian et al., 2017; Gilbert et al., 2018; Kääb et al., 2018).

The massive, sudden detachments of both the Kolka and Aru glaciers caused the loss of human lives (Evans et al., 2009; Tian et al., 2017). These two extreme events have been critical in posing relevant questions on the origin and dynamics of massive glacier collapses of low-angle glaciers and their implication for glacier-related hazards over other mountain areas worldwide (Kääb et al., 2005). The recent Caucasus and Tibet events also showed that glacier instabilities of catastrophic nature with no historical precedents can happen under specific circumstances. Previously known catastrophic glacier instabilities should be re-evaluated in the light of the new findings in order to investigate their relation to processes involved in the massive Caucasus and Tibet glacier collapses, or ice avalanching from steep glaciers, respectively (Kääb et al., 2018).

In this contribution we present the collapse of a cirque glacier in the Central Andes of Argentina in March 2007, which we informally named Leñas Glacier. Owed to the isolated location of the glacier and the lack of human activity affected, the event had remained unnoticed until recently (Falaschi et al., 2018a). Based on the analysis of aerial photos, high resolution satellite imagery, and field observations, we follow the evolution of the Leñas Glacier from the 1950´s through present day, describe the collapse event and later changes of the avalanche ice deposits, and discuss the possible triggering factors for the collapse. It should be noted that the remoteness of the study site, and the fact that the event remained unnoticed for a decade, limit the data base available to interpret the event. We consider it nonetheless important to report about this unusual glacier collapse in order to contribute to the discussion about glacier instabilities.

2 Study area

The Leñas Glacier (34º 28' S – 70º 3' W; lower limit ca. 3450 m asl.; Fig. 1a) is located at the headwaters of the Atuel river, in the Argentinean province of Mendoza. The climate in this portion of the Andes of Argentina and Chile has been described as a Mediterranean regime. Snowfall maxima occur during the austral cold season (April-October), as the westerly flow drives frontal systems eastwards from the Pacific Ocean over the Andes. Glaciers in the Central Andes have retreated significantly since the second half of the 20th century (Malmros et al., 2016). Specifically in the Atuel catchment, Falaschi et al. (2018a) reported a moderate (though highly variable) glacier thinning rate of 0.24 ±0.31 m a^{-1} overall for the 2000-2011 period.

Regarding glacier instability processes, there is a total of 16 glacier avalanches in the Tropical Andes of Peru and Colombia contained in the WGMS database, involving avalanche volumes of 0.2-100 × 10^6 m^3 (WGMS, 2017). In the classic work of Lliboutry (1956) on the glaciers of the Southern Andes, a number of ice break-offs in icefalls in the Central Andes of Chile are reported, though none of them were out of the ordinary in order to have raised particular consideration. More recently, at least two glaciers in Central Chile have lost a significant portion of their mass in sudden collapses (Iribarren Anacona et al., 2014), namely, the 7.2 × 10^6 m^3 detachment of a debris-covered glacier just south of Cerro Aparejo (33°34'S–70°00'W) in March 1980 (Marangunic, 1997), and the 1994 ice avalanche in the southern flank of Volcán Tinguiririca (34°48'S–70°21'W), merely 50 km southwest of the Leñas Glacier (Iribarren Anacona et al., 2014). A second, 10-14 × 10^6 m^3 ice-rock avalanche originating from Tinguiririca glacier occurred in January 2007 (Iribarren Anacona and Bodin, 2010; Schneider et al., 2011), only two months before the Leñas event.

The abundance of rock glaciers and perennial snow patches in the Leñas Glacier surrounding (Fig. 1a) indicates that permafrost is widespread in the area. Brenning (2005) indicated for the region that the minimum elevation of rock glacier fronts is indicative of negative levels of mean annual air temperature (MAAT) and of the altitudinal lower limit of discontinuous mountain permafrost, and set its extent at 3200 m in the nearby Cerro Moño range (34º 45' S; see also Brenning and Trombotto, 2006; Brenning and Azócar, 2010; Azócar and Brenning, 2010). This value is comparatively higher than the ~2800 m elevation established for the whole Atuel catchment by IANIGLA (2015). The rough global permafrost zonation index map (Gruber, 2012) also indicates probable permafrost around the Leñas Glacier.

Lithology in the glacier surroundings is chiefly composed of pre and post-glacial volcanics (basalts, andesites and dacites) of Pliocene and Holocene age. Glacial, fluvial and mass removal processes have eroded and transported these rocks, which form the glacier forefields and outwash plains.

3 Satellite imagery and field observations

During the five decades prior to the 2007 collapse, Leñas Glacier occupied a small glacier cirque, south below the rockwall of the Morro del Atravieso peak (4590 m) and had a short debris-covered tongue in the flatter terrain underneath (Figs.1a 2 a-c). The analysis of available aerial photos shows that the glacier had an area of ~2.24 km^2 in 1955, and had shrunk to ~2.15 km^2 by 1970. There was no further area decrease until 2007. Concomitantly, the front retreated some 200 m between 1955-2007. Before the collapse, the elevation range of the glacier spanned between 4555-3441 m.

Sometime between 5 March (Landsat image showing an intact glacier) and 14 March 2007 (SPOT5 image showing the collapse), the lowermost part (3630-3441 m) of the glacier detached from the main glacier and produced an ice avalanche that ran down the valley for ~2 km, measured from the uppermost part of the scarp to the most distant point of the fragmented ice mass (Fig. 1). Immediately after collapse, the ice avalanche had an area of 0.63 km^2 (Figs. 1, 2d). The orographic right (western) portion of the glacier subsided, but the break-off was restrained by a lateral moraine (Fig. 2a). The elevation difference between the scarp head and the avalanche terminus of only 190 m results in a low angle of reach of only 5º (i.e. the avalanche horizontal distance and its vertical path, the so-called 'Fahrböschung'). The failed glacier portion had an average surface slope of 15.6º (derived from the SRTM DEM) and an area of about 250,000 m^2 as measured from Quickbird imagery of 19 April 2007.

To estimate the avalanche volume we subtract the February 2000 1-arcsecond C-band SRTM DEM from the ALOS PRISM World DEM AW3D (Fig. 1c). For the SRTM DEM we assume no penetration of the radar pulse into the snowpack and ice as February 2000 falls in austral summer with melting conditions likely. The assumption of no to little radar penetration is confirmed by the fact that the C-band and the X-band SRTMs show no significant vertical difference over the Leñas and other glaciers in the area (cf. Gardelle et al. 2012) and that the SRTM image product shows for these glaciers low backscatter, a sign for surface melt (Kääb et al. 2018). The AW3D DEM is stacked from individual DEMs from ALOS

PRISM optical stereo triplets. Exploration of the PRISM archive shows that the first suitable scene of the study site is from 18 April 2007 (i.e. after the collapse), and there are good scenes for every year over 2007–2011. In the averaged DEM product AW3D the elevations should thus roughly represent the average year 2009. The differences between the 2000 SRTM and the ~2009 AW3D DEMs (Fig. 1c) reveal a volume loss over the collapse detachment area of 4.0 x 10^6 m^3. We also compute differences between the SRTM DEM and the TanDEM-X WorldDEM, the raw data of which were acquired between January 2011 and September 2014, giving an average date of ~2013. The volume change over the glacier detachment estimated from these DEMs is around 3.5 x 10^6 m^3. Our DEM-based estimates include, though, not only glacier elevation changes between 2000 and the collapse date in March 2007, but also changes between the 2007 collapse date and the date represented by the AW3D DEM, or the TanDEM-X DEM, respectively. Correcting for linear elevation loss between 2007 and ~2013 suggests thus a 2007 detachment volume of around 4.2 x 10^6 m^3. A volume error of ±0.3 x 10^6 m^3 was calculated according to Wang and Kääb (2015) using an off-glacier standard deviation of elevation differences found to be 2.3 m and a conservative autocorrelation length of 400 m. Assuming instead complete correlation of the elevation differences (i.e. assuming the number of observations n to be 1) gives a pessimistic volume uncertainty of ±0.6 x 10^6 m^3 or around 15% of the volume estimated. Incidentally, the positive elevation changes seen in the upper part of the glacier are most probably the result of DEM artifacts on steep terrain and due to different details included in the SRTM and AW3D DEMs (as becomes clear from visually comparing their hillshades), but have nevertheless no impact on the general pattern of the elevation trends observed here (see e.g. Le Bris and Paul, 2015).

For an independent check of the collapse volume, we estimate the average glacier thickness at the scarp to have been roughly 35 m as derived from scarp shadows and solar angles at the time of image acquisitions. Thus, assuming arbitrarily linear decrease of the glacier thickness from the scarp to the former glacier front, an average glacier thickness of 18 m yields a rough estimate of 4.5 x 10^6 m^3 of ice detached in the avalanche. This collapse volume agrees well with the above more quantitative estimate based on DEM differences.

The large crevasses that would later delineate the collapse scarp were clearly visible 3 weeks before the collapse (Fig. 2c) but strong crevassing at approximately the same location is also evident in the 1970 aerial photos (Fig. 2b). This indicates a potential break in slope of the glacier bed at this location. Interestingly, the upper, steeper part of the glacier that had been mainly devoid of rock debris before the collapse, gradually became debris covered after the break off (Fig. 2e,f). It is however unclear if this development is related to the collapse (e.g., due to debris concentration on a now flatter glacier), or coincidental (e.g., related to overall glacier shrinkage in the area, or increased rock fall activity from the steep mountain flank above the glacier).

The ice avalanche deposit transformed from a mostly clean-ice surface directly after the collapse in 2007 (Fig. 2d) to a debris-covered one later on (Fig. 2e-f, 3a). Ice interspersed with rocks is featured at the avalanche terminus in the 19 April 2007 Quickbird image (Fig. 2d) and by 2011, the full ice debris (as most of the upper portion of the glacier) had been sheltered by scree. Also, the detachment scarp and crevasses have disappeared, and large thermokarst ponds have formed within the avalanche deposit. Currently, the avalanche terminus lies ~450 m horizontally up the valley with respect to the maximum avalanche extent in 2007.

The ice deposits of the Leñas collapse sit on a flat leveled plateau consisting of volcanic rocks, reworked by glacial erosion, rockfall and maybe previous collapses. As stated above, the ice avalanche is meanwhile fully debris covered, though massive ice is visible on the walls of thermokarst ponds and ice cliffs. Within the avalanche deposit, which has now mostly a subdued and concave topography, at least two small outwash plains are forming, one at the abrupt slope change just above the uppermost reaches of the avalanche deposit, the other in front of the avalanche terminus (Fig. 3a).

Recent field observations of the detachment area done in March 2018 confirmed the absence of a hard bedrock underneath the glacier, as already suggested by the high-resolution satellite images. The sediment layer beneath the failed glacier area is deeply incised with gullies showing no hard bedrock (Fig. 3a,b) Also, the terrain under the former avalanche scarp is steep and not too rough (see Fig. 3a). Further down, debris in the ice avalanche deposit is composed of fragments of volcanic rock (<0.5 m in size) contained in a finer (pelitic to sandy) matrix, and very few large boulders (Fig. 2a,c). We assume this material to be further evidence of the soft bed upon which the glacier rested before collapse. Between the outer limit of the ice avalanche and the LIA moraines (Fig. 1a, 3d), the terrain is made up of a chaotic arrangement of hummocks and thermokarst ponds that appear similar (though smoother) to the complex topography of the actual avalanche deposit (Fig. 3a). From the 2018 terrain inspection, and the 1955 and 1970 aerial photographs from before the collapse, it appears that the ice avalanche flowed over a seemingly bumpy, rough surface.

4 Meteorological and seismic data

We used the CHIRPS daily precipitation data (Funk et al., 2015), with a spatial resolution of 0.05° to identify unusually high rainfall occurrences. During the period 4-15 March 2007, no precipitation was recorded in the CHIRPS pixel where the Leñas collapse occurred and its surrounding pixels. These results were further verified with data from in-situ observations from the Laguna Atuel meteorological station. In addition, daily temperature reanalysis fields from ERA-Interim (Dee et al., 2011) were analyzed, considering the anomalies over the study area based on the 1981-2010 standard period. Results show that temperature anomalies close to 3°C above normal were recorded during 11 and 12 March 2007.

Using data from the USGS earthquake catalogue (http://earthquake.usgs.gov) and applying the ground acceleration criteria discussed in Kääb et al. (2018) we find no earthquake between 4 and 15 March 2007 that could have triggered the Leñas collapse. The strongest earthquake found during the period of concern and within a radius of 1000 km had a magnitude of 5.0 and distance of about 200 km from Leñas (depth 35 km; 11 March). The closest earthquakes (20-30 km) had magnitudes of 2.5 (4 March, 8.3 km depth) and 3.2 (11 March, 128 km depth).

6 Discussion

In terms of volume, and glacier and runout slopes, the type of the 2007 Leñas Glacier collapse (4.2 x 10^6 m^3) seems to range somehow in between ice avalanches from steep hanging glaciers (>30º) and the massive collapses of 2002 in the Caucasus and 2016 in Tibet. Compared to the Kolka (130 × 10^6 m^3; Evans et al., 2009) and Aru (68 ±2 × 10^6 m^3 and 83 ±2 × 10^6 m^3; Kääb et al., 2018) collapses, the Leñas event has a much smaller mass of ice sheared off due to a smaller and shallower glacier. On the other hand, despite the spatial and temporal proximity, the Leñas and Tinguiririca events are probably different in nature. In the first place, the Tinguiririca event involved a much larger volume (10-14 × 10^6 m^3 vs. 4.2 × 10^6 m^3 -Schneider et al., 2011) and secondly, the head slope is a bit higher (~20º vs. 15.6º). On another note, the 2007 Leñas event is also not typical for regular ice avalanches as the glacier was not very steep (15.6º) and the event volume is at the upper margin of more typical ice break-offs (Failletaz et al. 2015; Alean, 1985).

An important finding from field work is the abundance of fine sediments in and on the collapse deposits (Fig. 3). We suggest that a soft glacier bed material could have played an important role in the collapse enhancing avalanche mobility, as already noted for the Kolka and Aru collapses (Gilbert et al., 2018). Also, the rather large amount of debris on top of the collapse deposits has probably favored the rather good preservation of much collapse ice, even 11 years after the event took place. In comparison, the bare ice deposits of the Aru glacier collapses will have melted away to a large extent 2 years after collapse whereas the heavily debris-covered and up to more than 100 m thick deposits of the Kolka glacier collapse lasted many years despite their low elevation (Kääb et al., 2018),

As potential factors for large glacier collapses, a number of causes have been investigated so far, namely (i) high liquid water input into the glacier system from precipitation and melting, (ii) seismicity, (iii) changes in glacier geometry, and (iv) a shift in the thermal regime towards warmer conditions (Gilbert et al., 2018; Kääb et al., 2018). In the first place, our analyses of meteorological data showed no evidence of unusually strong increases in precipitation or temperature in the days immediately preceding the Leñas collapse that would directly destabilize the glacier. Neither do earthquake records reveal any strong seismic activity that could have triggered the collapse. Instability may be favored as a glacier recedes from a flatter foot back into a steeper part of the bed, loosing thus the fontal stabilization in a type of self-debuttressing process, as also found for some more typical ice break-off situations (Faillettaz et al., 2015). From the very slight glacier area decrease in the Leñas case (2.24 to 2.15 km^2) before collapse, we cannot identify a significant change in glacier geometry that would have changed its stress regime, but this finding could in parts be due to the limited availability of suitable DEMs. The Aru twin collapses in Tibet were preceded by geometry changes in the form of surge-like behavior (Kääb et al., 2018). Although surges in this region of the Andes and in close proximity to the Leñas Glacier have been documented Falaschi et al. (2018b), we were unable to detect any evidence of a surge leading to collapse in the satellite imagery and DEMs. As for a change in thermal regime, from the rock glaciers in the area and the long preservation of the collapse deposits we conclude a potentially cold ground temperature regime for parts of the glacier and forefield. The thin glacier front could have been frozen to the bed, and we cannot exclude that a change in this polythermal regime may have caused changes in stability.

We hypothesize a mixed origin for the debris layer observed on the ice avalanche deposit. On the glacier head, frost action and permafrost thaw are probably responsible for the production of fine grained deposits originating from rock fall off the steep and ice-free surrounding rock walls (Fig. 2, panels e and

f). The compact pieces of ice with a small amount of debris on top of them (Fig. 3b) may be intact parts of the former debris-covered glacier front that detached as a whole (or in few large fragments) and formed the front of the collapsed ice mass (cf. Fig. 1b, 2d). The loss of the glacier front likely debuttressed higher (and not debris-covered) glacier parts that came down after the front, either in direct sequence or even with some delay, in the latter case suggesting the possibility for different phases of the collapse with different properties. The former glacier front might have also ploughed through the forefield and in parts have taken up debris there together with the original debris cover on the glacier front. Although from the data accessible to us we cannot tell if the Leñas 2007 avalanche happened as one or few larger events (as also the Kolka and the second Aru event -Evans et al., 2009; Kääb et al., 2018), the morphology of the deposits and the low Fahrböschung nevertheless seem to exclude that the deposits are the product of repeated small ice falls.

6 Conclusions

In the region of the Central Andes studied here, gravity-driven failures of steep glaciers have been observed previously. The volume of the Leñas collapse of ~4 x 10^6 m^3 and the detachment slope of 15.6º, however, deviate from the more typical ice avalanches from steep glaciers and place the event closer to low-angle glacier collapses. Due to the large time lag between the Leñas Glacier collapse in 2007 and its discovery, and the remoteness of the site, only limited data are available to analyze the case. We are not able to identify a clear potential trigger of the Leñas event, as neither the meteorological or seismic data reveal unusual conditions or events that could have triggered the Leñas collapse, nor a significant change in glacier geometry before collapse could be identified. The event does not rule out the importance of soft bed characteristics as a factor in the (rare) collapses of low-angle glaciers (Kääb et al., 2018; Gilbert et al., 2018). Despite the knowledge deficiencies related, for instance, to the hydrological, hydraulic, or ground-thermal conditions under which the Leñas Glacier collapse took place, the information presented here adds to the spectrum of environmental and glaciological circumstances under which glacier collapses can take place, including related implications for mountain hazard management.

Author contribution

DF led and designed the study, conducted the field work, analyzed data, and wrote the paper. AK and FP helped in designing the study, analyzed data, and wrote the paper. TT processed and orthorectified the ALOS PRISM imagery. JAR prepared and analyzed the meteorological station and reanalysis data. LL helped in designing the study.

Competing interests

The authors declare that they have no conflict of interest.

Data availability

Landsat data and the SRTM C-band DEM are available from http://earthexplorer.usgs.gov, SRTM images from https://earthdata.nasa.gov/. The SRTM X-band DEM is available from http://eoweb.dlr.de, the TanDEM-X WorldDEM from https://geoservice.dlr.de/web/ The ALOS AW3D is available from http://www.eorc.jaxa.jp/ALOS/en/aw3d30/. Earthquake data are available from http://earthquake.usgs.gov. Data from DigitalGlobe (Quickbird), Planet, and Airbus (SPOT) are commercial.

Acknowledgements

The present study was carried out in the framework of the SeCTyP project *Investigación, a partir de las Aplicaciones Geomáticas de los cambios recientes en los ambientes glaciarios relacionados con la variabilidad climática en las cuencas superior del Río Mendoza y del Río Atuel* from the Universidad Nacional de Cuyo, Argentina.

The authors would like to thank Dario Trombotto (IANIGLA) for his comments on permafrost and Mariana Correas Gonzalez, Andrés Lo Vecchio (IANIGLA) and the *baqueano* Saul Araya for assistance during field work. Andreas Kääb acknowledges support by the European Research Council under the European Union's Seventh Framework Programme (FP/2007–2013)/ERC grant agreement no. 320816, and the ESA projects Glaciers_cci (4000109873/14/I-NB) and DUE GlobPermafrost (4000116196/15/IN-B). The comments of Fabian Walter and two further anonymous referees were pivotal for a better presentation of this work's content.

References

Alean, J.: Ice avalanches: some empirical information about their formation and reach, Journal of Glaciology, 31(109), 324-333, 1985.

Azócar, G. F., and Brenning, A.: Hydrological and geomorphological significance of rock glaciers in the dry Andes, Chile (27°–33°S), Permafrost and Periglacial Processes, 2, 42-53, doi:10.1002/ppp.669, 2010.

Brenning, A.: Geomorphological, Hydrological and Climatic Significance of Rock Glaciers in the Andes of Central Chile (33-35º S), Permafrost and Periglacial Processes, 16, 231-240, doi:10.1002/ppp.528, 2005.

Brenning, A., and Azócar, G. F.: Statistical analysis of topographic and climatic controls and multispectral signatures of rock glaciers in the dry Andes, Chile (27°–33°S), Permafrost and Periglacial Processes, 21, 54-66, doi:10.1002/ppp.670, 2010.

Brenning, A., and Trombotto, D. : Logistic regression modeling of rock glacier and glacier distribution: Topographic and climatic controls in the semi-arid Andes, Geomorphology, 81(1–2), 141-154, doi:10.1016/j.geomorph.2006.04.003, 2006.

Dee, D. P., and 35 others, 2011: The ERA-Interim Reanalysis: Configuration and performance of the data assimilation system, Quart. J. Roy. Meteor. Soc., 137, 553–597, doi:10.1002/qj.828.

Evans, S. G., Tutubalina, O. V. Drobyshev, V. N., Chernomorets, S. S., McDougall, S., Petrakov, D. A., and Hungr, O.: Catastrophic detachment and high-velocity long-runout flow of Kolka Glacier, Caucasus Mountains, Russia in 2002, Geomorphology, 105(3–4), 314-321, doi:10.106/j.geomorph.2006.10.008, 2009.

Faillettaz, J., Funk, M., and Vincent, C.: Avalanching glacier instabilities: Review on processes and early warning perspectives, Rev. Geophys., 53, 203–224, doi:10.1002/2014RG000466, 2015.

Falaschi, D., Lenzano, M. G., Tadono, T., Vich, A. I., and Lenzano, L. E.: Balance de masa geodésico 2000-2011 de los glaciares de la cuenca del río Atuel, Andes Centrales de Mendoza (Argentina), Geoacta, 42(2), 7-22, 2018a.

Falaschi, D., Bolch, T., Lenzano, M. G., Tadono, T., Lo Vecchio, A., and Lenzano, L.: New evidence of glaciar surges in the Central Andes of Argentina and Chile, Progress in Physical Geography, 42(6), 792-825, doi: 10.1177/0309133318803014, 2018b..

Funk, C., Peterson, P., Landsfeld, M., Pedreros, D., Verdin, J., Shukla, S., Husak, G., Rowland, J., Harrison, L., Hoell, A., and Michaelsen, J.: The climate hazards infrared precipitation with stations - a new environmental record for monitoring extremes, Sci. Data 2, 150066, doi:0.1038/sdata.2015.66, 2015.

Gardelle, J., Berthier, E., and Arnaud, Y.: Impact of resolution and radar penetration on glacier elevation changes computed from DEM differencing, Journal of Glaciology, 58, 419-422, 10.3189/2012JoG11J175, 2012.

Gardelle, J., Berthier, E., Arnaud, Y., and Kääb, A.: Region-wide glacier mass balances over the Pamir-Karakoram-Himalaya during 1999–2011, The Cryosphere, 7, 1263–1286, doi:10.5194/tc7-1263-2013, 2013.

Gilbert, A., Leinss, S., Kargel, J., Kääb, A., Yao, T., Gascoin, S., Leonard, G., Berthier, E., and Karki, A.: Mechanisms leading to the 2016 giant twin glacier collapses, Aru range, Tibet, The Cryosphere, 12, 2883-2900, doi:10.5194/tc-12-2883-2018, 2018.

Gruber, S.: Derivation and analysis of a high-resolution estimate of global permafrost zonation, The Cryosphere, 6, 221-233, doi:10.5194/tc-6-221-2012, 2012.

IANIGLA: Informe de la Cuenca del río Atuel, Provincia de Mendoza. IANIGLA-CONICET, Secretaría de Medio Ambiente y Desarrollo Sustentable de la Nación, Argentina, 67 pp, 2015.

Iribarren Anacona, P., and Bodin, X.: Geomorphic consequences of two large glacier and rock glacier destabilizations in the Central and Northern Chilean Andes, Geophysical Research Abstracts, 12, 7162–7165, 2010.

Iribarren Anacona, P., Mackintosh, A., and Norton, K. P.: Hazardous processes and events from glacier and permafrost areas: lessons from the Chilean and Argentinean Andes, Earth Surf. Process. Landforms, 40, 2–21, doi:10.1002/esp.3524, 2014.

Kääb, A., Berthier, E., Nuth, C., Gardelle, J., and Arnaud, Y.: Contrasting patterns of early twenty-first-century glacier mass change in the Himalayas, Nature, 488, 495–498, doi:10.1088/nature11324, 2012.

Kääb, A., Huggel, C., Fischer, L., Guex, S., Paul, F., Roer, I., Salzmann, N., Schlaefli, S., Schmutz, K., Schneider, D., Strozzi, T., and Weidmann, Y.: Remote sensing of glacier- and permafrost-related

hazards in high mountains: an overview, Natural Hazards and Earth System Sciences, 5, 527–554, 2005.

Kääb, A., and 18 others, Massive collapse of two glaciers in western Tibet in 2016 after surge-like instability, Nature Geoscience, 11, 114–120, doi:10.1038/s41561-017-0039-7, 2018.

Le Bris, R., and Paul, F.: Glacier-specific elevation changes in parts of western Alaska, Annals of Glaciology 56(70), 184-192, doi:10.3189/2015AoG70A227 , 2015.

Lliboutry, L.: Nieves y glaciares de Chile, fundamentos de glaciología, Universidad de Chile, Santiago de Chile, 472 pp., 1956.

Marangunic, C.: Deslizamiento catastrófico del glaciar en el Estero Aparejo, in: Actas del 4° Congreso Chileno de Geotecnia, 2, 617–626, 1997.

Tian, L., Yao, T., Gao, Y., Thompson, L., Mosley-Thompson, E., Muhammad, S., Zong, J., Wang, C., Shengqiang, J., and Zhiguo, L.: Two glaciers collapse in western Tibet, Journal of Glaciology, 63(237), 194-197, doi:10.1017/jog.2016.122, 2017.

Rowan, A. V., Egholm, D, L., Quincey, D. J., and Glasser, N. F.: Modelling the feedbacks between mass balance, ice flow and debris transport to predict the response to climate change of debris-covered glaciers in the Himalaya, Earth and Planetary Science Letters, 430, 15, 427-438, doi:10.1016/j.epsl.2015.09.004, 2015.

Schneider, D., Huggel, C., Haeberli, W., and Kaitna, R.: Unraveling driving factors for large rock–ice avalanche mobility, Earth Surface Processes and Landforms, 36, 1948-1966, doi:10.1002/esp.2218, 2011.

Wang, D., and Kääb, A.: Modeling glacier elevation change from DEM time series, Remote Sensing, 7(8), 10117-10142, doi:10.3390/rs70810117, 2015.

WGMS: Global Glacier Change Bulletin No. 2 (2014-2015), Zemp, M., Nussbaumer, S. U., Gärtner-Roer, I., Huber, J., Machguth, H., Paul, F., and Hoelzle, M. (Eds.), World Glacier Monitoring Service, Zurich, Switzerland, 244 pp., 2017.

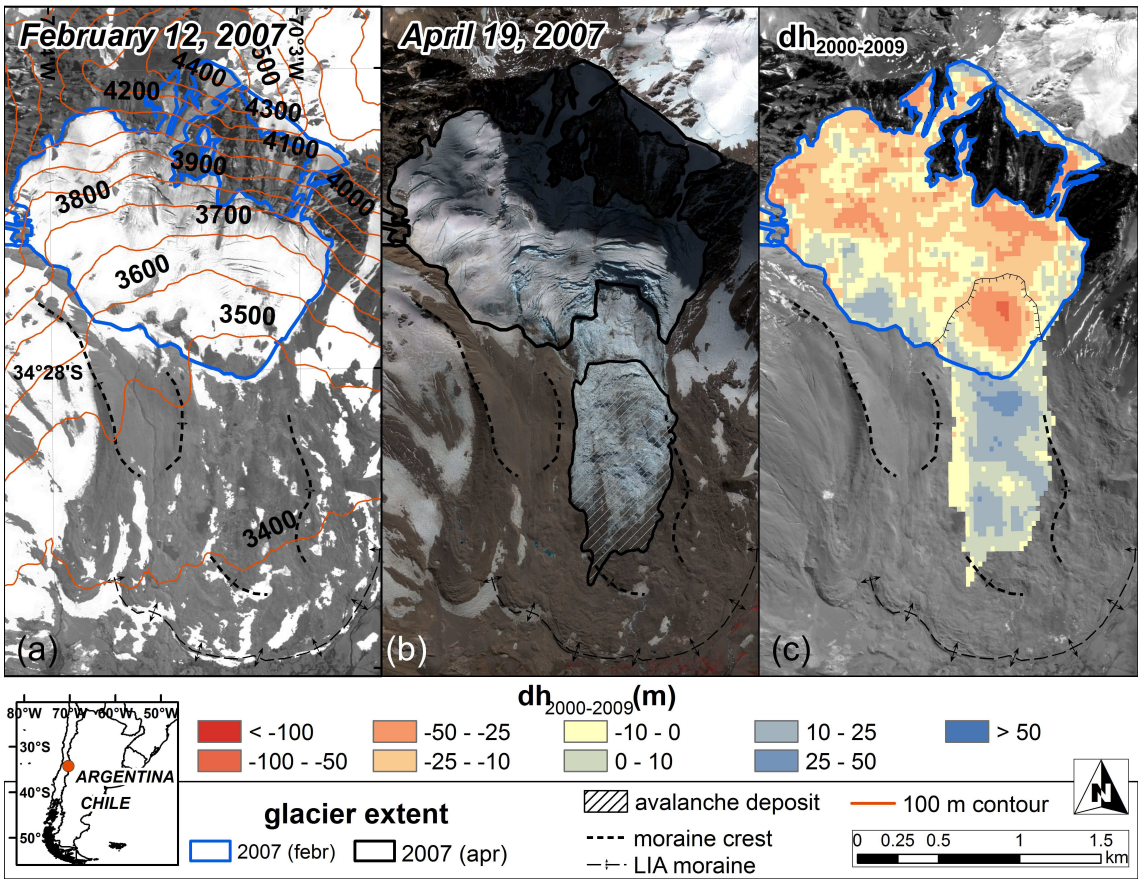

Figure 1: (a) The Leñas Glacier before (SPOT 5, 12 February 2007) and (b) after collapse (Quickbird image - RGB 432- 19 April 2007). (c) 2000-2009 elevation differences (background image ALOS PRISM, 31 March 2011). Inset: Location of the Leñas Glacier in the study area.

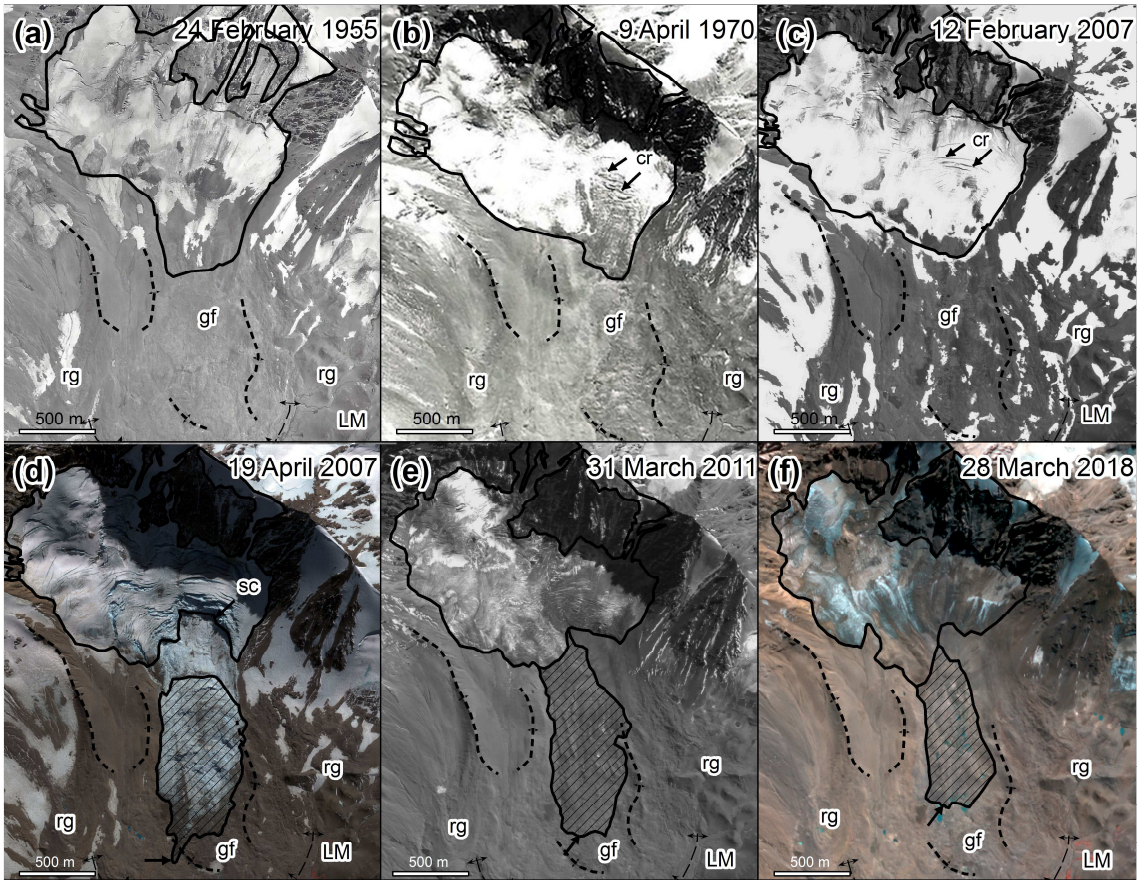

Figure 2: Evolution of the Leñas Glacier (black line) and avalanche deposit extent through time. (a,b) –aerial photos- and (c) -SPOT 5- show the glacier's slight retreat before collapse. The large crevasses visible in the 1970 (b) and February 2007 (c) demark the location of the scarp head in the Quickbird scene of 19 April 2007 (d). (e) -ALOS PRISM) and (f) –Planet RGB 432- depict the growth of debris-covered portions on the glacier and the transformation of the collapse deposits. The black arrow shows the distal terminus of the avalanche deposit. gf: glacier forefield LM: LIA moraine rg: rock glacier cr: crevasse sc: avalanche scarp

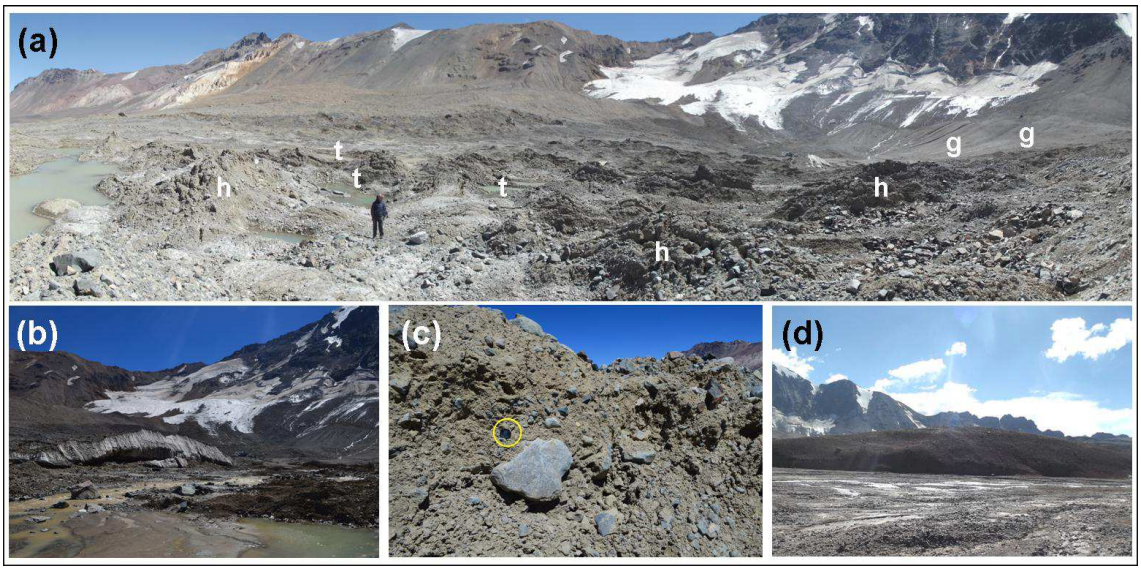

Figure 3: (a) Panoramic view of the Leñas Glacier and avalanche deposit in March 2018, showing the chaotic arrangement of thermokarst ponds (t) and hummocks (h), and the glacier head on the far upper right. The failed glacier area lies below the debris-free ice. Note the absence of rock outcrops/hard bed in the failed glacier area and the deeply incised gullies (g) in the sediment layer. (b) Former glacier fragment at the base of the detachment area arrow in Fig. 3). (c) Detail of the debris cover on the avalanche deposit, showing the rock fragments and matrix (see the black camera objective cover inside the yellow circle for scale). (d) Presumably ice-cored LIA moraines. Photos (b) and (c) courtesy Mariana Correas.